SCIENTIFIC REPORTS

OPEN

SUBJECT AREAS:
NANOPHOTONICS
NANOTECHNOLOGY
OPTICAL MATERIALS AND STRUCTURES
SYNTHESIS

Received
8 July 2011

Accepted
22 September 2011

Published
10 October 2011

Correspondence and requests for materials should be addressed to Q.K.X. (qkxue@mail.tsinghua.edu.cn) or M.W.C. (mwchen@wpi-aimr.tohoku.ac.jp).

* These authors contributed equally to this work.

Single molecule detection from a large-scale SERS-active $Au_{79}Ag_{21}$ substrate

Hongwen Liu[1]*, Ling Zhang[1]*, Xingyou Lang[1], Yoshinori Yamaguchi[2,3], Hiroshi Iwasaki[2,3], Yasushi Inouye[2], Qikun Xue[1,4] & Mingwei Chen[1,5]

[1]WPI-Advanced Institute for Materials Research, Tohoku University, Sendai 980-8577, Japan, [2]Department of Applied Physics, Graduate School of Engineering, Osaka University, Osaka 565-0871, Japan, [3]PARC, Graduate School of Engineering, Osaka University, Osaka 565-0871, Japan, [4]Department of Physics, Tsinghua University, Beijing 100084, China, [5]State Key Laboratory of Metal Matrix Composites, School of Materials Science and Engineering, Shanghai Jiao Tong University, Shanghai 200030, China.

Detecting and identifying single molecules are the ultimate goal of analytic sensitivity. Single molecule detection by surface-enhanced Raman scattering (SM-SERS) depends predominantly on SERS-active metal substrates that are usually colloidal silver fractal clusters. However, the high chemical reactivity of silver and the low reproducibility of its complicated synthesis with fractal clusters have been serious obstacles to practical applications of SERS, particularly for probing single biomolecules in extensive physiological environments. Here we report a large-scale, free standing and chemically stable SERS substrate for both resonant and nonresonant single molecule detection. Our robust substrate is made from wrinkled nanoporous $Au_{79}Ag_{21}$ films that contain a high number of electromagnetic "hot spots" with a local SERS enhancement larger than 10^9. This biocompatible gold-based SERS substrate with superior reproducibility, excellent chemical stability and facile synthesis promises to be an ideal candidate for a wide range of applications in life science and environment protection.

Surface-enhanced Raman scattering (SERS) is one of the few techniques[1–4] that are capable to reach analytical limit. SERS-based single molecule detection (SM-SERS)[1,5–12] is mostly achieved from silver colloidal nanoparticles that are randomly deposited on glass or silicon substrates. Very low molecule concentrations ($< 10^{-8}$ M) are usually chosen to ensure that statistically there is no more than one molecule per colloid, and that the Raman signal originating from the sample can be considered from a single molecule. Large electromagnetic fields for SM-SERS are typically generated at the junction between nanoparticles (namely "hot spots"). Extensive studies have recently focused on creating "hot spots" or boosting SERS-active sites on colloidal nanoparticles[7–9,13,14], such as in nanogaps[7], or in the nanofabrication of silver heterodimers[8], star-like nanoparticles[9], and oxide shell-isolated nanoparticles[14]. The main problems with colloidal particles are their poor structural reproducibility and the easy oxidation and sulfuration of silver nanoparticles. To control and immobilize SERS-active sites, advanced lithographic techniques have succeeded in optimizing well-ordered arrays of silver-dimer[15] and bowtie-nanoantenna[16]. These devices show a large Raman enhancement ability but not SM-SERS. One possible reason is that the maximum enhancement of the local field at the minimum scale with these "top-to-down" approaches is still insufficient for single-molecule detection. Other attempts for developing high-performance SERS substrates include the use of poly(vinyl alcohol) fibers[17] or three-dimensional (3D) nanoporous alumina membranes[18] to carry SERS-active nanoaggregates. The shortcoming of these techniques is that the fabrication procedure is very complicated and the SERS performance relies on the quality of both the membranes and the nanoparticles. To the best of our knowledge, there is no report on large scale and free-standing SERS-active films with single molecule Raman resolution.

It has been known for decades that nanoporous metal films with a bicontinuous network structure can be synthesized by a dealloying method[19,20], but their superior optical properties in SERS have been demonstrated only very recently[21,22]. Strong electromagnetic fields appear in the vicinity of metallic ligaments due to the large curvatures of the nano-sized ligaments and nanopores, as well as the electromagnetic coupling between the neighbour ligaments[23]. Easy synthesis and large film size promote dealloyed nanoporous metal films as effective SERS-active substrates. However, their in-plane structural features and smooth ligament surfaces resulted from chemical etching constrain the local electromagnetic field strength below the limit for SERS-based single molecule

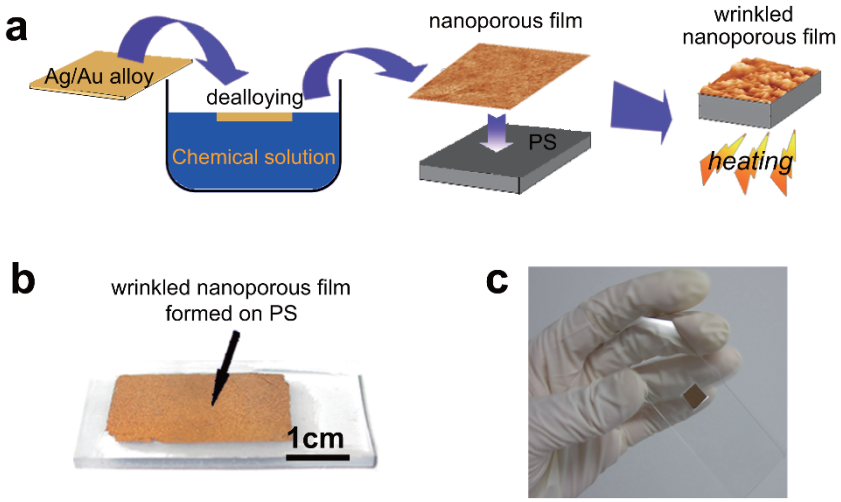

Figure 1 | Wrinkled nanoporous substrate. (a) Schematic diagram of the preparation of wrinkled nanoporous films. (b) Photograph of a plasmonic substrate consisting in a wrinkled nanoporous film with dimensions 30 mm × 15 mm supported on a polymer substrate. (c) Photograph of the substrate used in this work with dimensions of 8 mm × 8 mm.

detection[21–23]. The SERS performances of nanoporous metal films can be further improved by introducing 3D quasi-periodic wrinkles through thermal contraction of pre-strained polymer substrates (**Fig. 1a**)[24–26]. Using this procedure detailed in the Method section, rich SERS-active nanostructures at the ridges of the wrinkles, such as nanogaps and nanotips, are produced by deformation and failure of metal ligaments during film shrinking. The dimension of the wrinkled substrates can be discretionarily changed from several micrometres to tens of centimetres ready for direct device applications (**Fig. 1b and c**). In this study, we demonstrate that SM-SERS for both resonant and nonresonant molecules can be readily achieved from a robust, chemically stable and large-scale SERS-active wrinkled nanoporous $Au_{79}Ag_{21}$ alloy film substrate.

Results

The microstructure of the as-prepared nanoporous film used in this study is illustrated in **Fig. 2a**. As shown in the low-magnification scanning electron microscopy (SEM) image, the as-prepared film is flat before wrinkling treatment. The dealloyed film possesses bicontinuous nanoporosity and free etching leads to nanopores and ligaments nearly identical in size, geometry and topology (**Fig. 2a** inset). Quasi-periodic wrinkles formed by annealing distribute uniformly across the entire film (**Fig. 2b**). The biaxial wrinkling gives rise to rose-petal-shape nanostructures, as shown in the inset of **Fig. 2b**. According to chemical composition analysis, the nanoporous film contains more gold than silver after dealloying, in a proportion of 71:29 (at. %) (**Fig. 2c**). It is worth noting that the wrinkling treatment

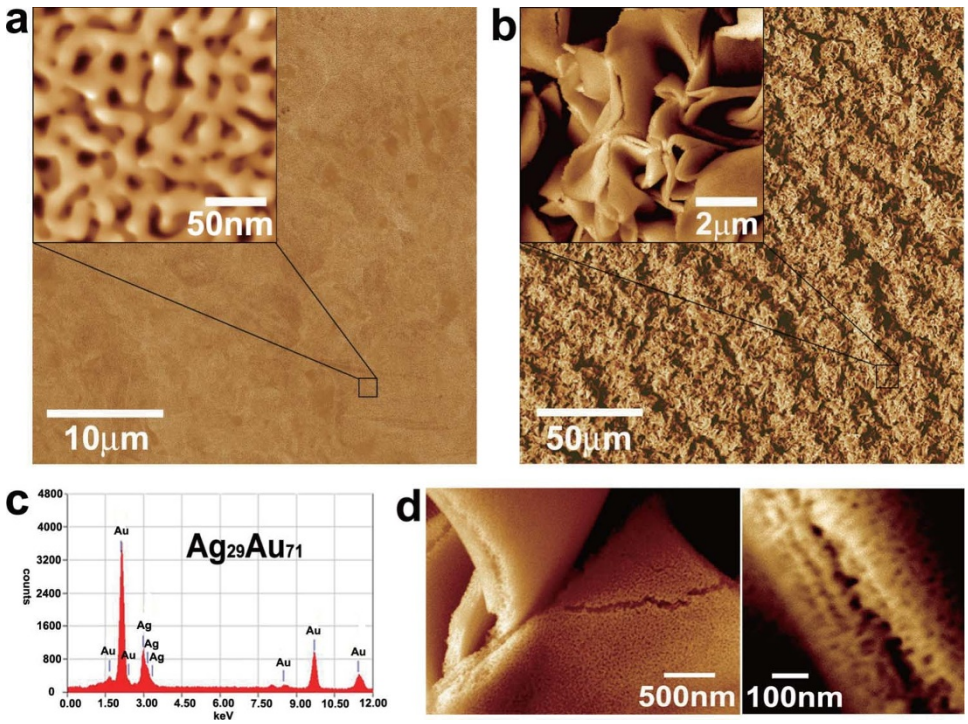

Figure 2 | Microstructure characterization of wrinkled nanoporous films. (a) SEM micrographs of the flat nanoporous film with a characteristic length of 20 ~ 25 nm. (b) Microstructure of a wrinkled nanoporous film with a quasi-periodic wavelength of 10 ~ 15 μm. (c) Chemical composition of a nanoporous film measured by energy dispersive X-ray spectroscopy. (d) Microstructure of wrinkle ridges showing nanogaps, interleaving broken ligaments and linear chains of self-similar nanocavities.

does not cause any obvious change in the nanoporosity of the wrinkled nanoporous film except for a slight coarsening of the nanopores and the gold ligaments. Owing to the large deformation caused by wrinkling, cracks are frequently observed along the ridges of wrinkles (**Fig. 2d**), which form nanogaps by interleaving fractured gold ligaments with various spaces from smaller than one nanometre to tens of nanometres.

We first demonstrate the SERS efficiency of the wrinkled nanoporous film by comparing average Raman intensities of active fluorescent molecules of R6G deposited on the flat nanoporous film and the wrinkled one. As illustrated in **Fig. 3a**, Raman signals are undetectable for R6G with 1×10^{-10} M concentration on the flat film. However, intense characteristic Raman bands of R6G at the same concentration emerge on the wrinkled film. Even when the R6G solution is further diluted to 1×10^{-12} M, the characteristic bands of R6G are still clearly visible. The Raman mapping image shows wrinkle patterns due to the enhancement of the Raman signals along with the fluorescence background from bright ridges (**Fig. 3b**). The overlay (**Fig. 3c**) of the Raman mapping with the corresponding optical microscopic image indicates that the strongest enhanced signals are mostly from broken wrinkle ridges. Since Raman scattering is an extremely inefficient process with a cross section ($\sim10^{-30}$ cm^2 per molecule) ~14 orders of magnitudes smaller than that of florescence from the chromospheres with large quantum yields ($\sim10^{-16}$ cm^2 per molecule)[1], the SERS signal is comparable with normal fluorescent signal only at ultra high SERS enhancement. Unlike fluorescence signals, SERS is rich of molecular information provided from light scattered from very local and confined fields ("hot spots" which are about 1 μm^2 size in this study and identified by Raman fingerprints). Even at 10^{-10} M, a typical SERS spectrum with plenty of peaks recorded from a single hot spot (**Fig. 3d**) suggests ensemble molecules in the probe region[27].

Typical single-molecule SERS spectra from hot spots are shown in **Fig. 3d** for 10^{-12} M R6G (~0.25 molecules per μm^2, see the Method Section). In contrast to 10^{-10} M R6G, only selective peaks with narrower linewidth are visible in each spectrum. While these peaks differ from site to site in frequencies, relative intensities and linewidth, they can all be assigned to vibrational bands of R6G (see the Supplementary Information), demonstrating a common signature of single molecule detection[1,6,27]. In the case of a molecule ensemble, the characteristic SERS spectra are nearly identical from site to site since a large number of molecules with various orientations contribute to the accumulated SERS spectra.

The intensity of 28 hot spots for 10^{-12} M R6G molecules is reported in the inset of **Fig. 3d**. Most hot spots have a similar enhancement factor, but about 1/10 hot spots show an enhancement higher by more than one order of magnitude. The average enhancement factor of the wrinkled nanoporous $Au_{79}Ag_{21}$ film is estimated to be $\sim3\times10^8$ (see the Supplementary Information), which is about 4 times higher than that of wrinkled nanoporous pure gold[26]. In our Raman imaging measurements, the intensity of a hottest spot is ~500 times stronger than the average, indicating that the maximum enhancement factor of local fields on the wrinkled nanoporous $Au_{79}Ag_{21}$ film is as high as $\sim10^{10}$–10^{11}. The ultrahigh SERS enhancement from the wrinkled substrate is most likely from the superposition of the high electric field strength at the molecule (so-called electromagnetic effect) and the molecular polarizability (so-called chemical enhancement). The intensity fluctuation of scattering modes in each Raman spectrum for 10^{-12} M R6G (Fig. 3d) is related to the specific orientation of the molecule with respect to the laser

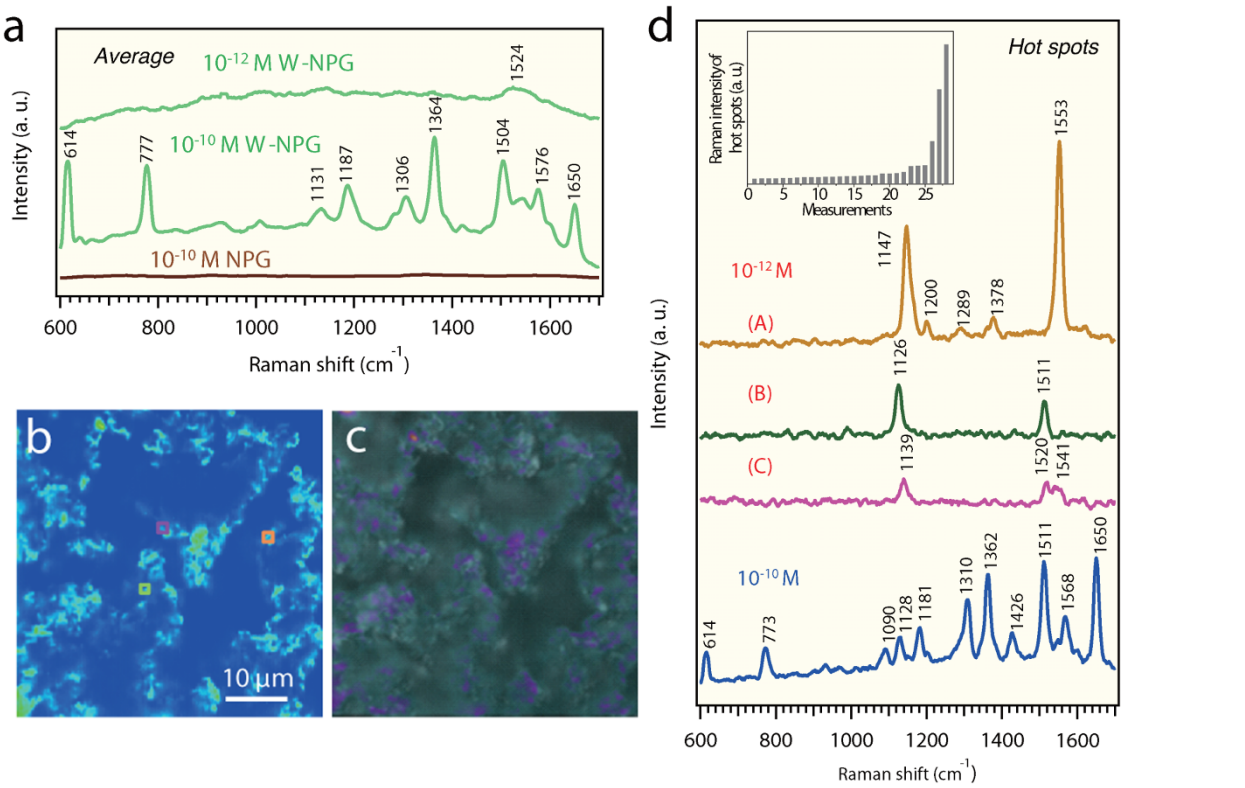

Figure 3 | Single molecule detection of R6G molecules. (a) Raman spectra of R6G from a flat nanoporous $Au_{79}Ag_{21}$ film and wrinkled one. (b) Typical Raman map of R6G (10^{-12} M) on the wrinkled $Au_{79}Ag_{21}$ film. The pixel size in the Raman map is 250 × 250 nm^2. (c) Overlay of the image in **b** and the corresponding optical microscopic image. The hot spots can be identified along the broken gaps of the wrinkled nanoporous film. (d) Typical SERS spectrum (blue) taken from a hot spot for 10^{-10} M R6G. Single molecule SERS spectra (A) (B) (C) for 10^{-12} M R6G taken from the three hot spots in the same colour squares in **b**. The inset in **d** gives the statistical distribution of Raman intensity of 28 hot spots in a Raman map of 10^{-12} M R6G. The laser excitation is 532 nm.

beam polarization[28], and the predominant peaks are associated with the individual adsorption status of the detected single molecules.

To further confirm the suitability of the wrinkled nanoporous film for single molecule SERS detection, we investigate an optically non-resonant bio-molecule: DNA nucleobase adenine. Due to their electrical neutrality in solution, a much smaller number of adenine molecules adsorb onto the nanoporous $Au_{79}Ag_{21}$ surface compared to R6G. In this study we chose a 785 nm excitation laser with which adenine molecules are not resonant. A typical Raman map of 10^{-9} M adenine is shown in **Fig. 4a**. The overlay of the Raman map and the optical microscopic image shows more clearly that the most active sites locate at the narrow broken ridges of the wrinkled nanoporous film. We believe that these "hottest spots" are associated with the coupled tips of fractured ligaments at the nanogaps, as shown in **Fig. 2d**. For a pair of tip-to-tip nanostructure with a small gap, the field enhancement due to the coupling effect can be 1000 times larger than that of an isolated one[29]. Computer simulations suggest that a linear chain of several metal particles or self-similar nanocavities creates spectrally and spatially configurable "superlenses" as resonant amplifiers and nanoconcentrators[30]. Interestingly, the "superlenses" can be frequently observed along the ridges of the wrinkled film (**Fig. 2d**). They can also act as the "hottest spots" responsible for the giant Raman scattering enhancement illustrated in the inset of **Fig. 4b**.

Similarly to the result for R6G, several characteristic Raman modes of adenine are visible for a concentration of 10^{-9} M (**Fig. 4c**), while only a few selective Raman bands appear when the concentration decreases to 10^{-12} M (**Fig. 4d**) (see the Supplementary Information). We rinsed the sample by large amount of water to remove the adenine molecules close to zero in any record pixel. Yet, Raman signals of adenine are still observed at few broken ridges of the wrinkles though the detectable hot spot number decreases dramatically. The extremely dilute-molecule detection at the single-molecule level appears to result from dominant local plasmon fields. In this case, the concentration of molecules is not the most important factor for detection. What really matters is that molecules reside at "hot spots".

Discussion

The density of hottest spots for SM-SERS detection in the wrinkled nanoporous film is estimated to be ~0.032 per μm² for 10^{-12} M of R6G in a Raman map. This value could be underestimated because molecules may not cover all SERS-active sites with the 10^{-12} M R6G concentration. Using colloidal particles, a quantitative measurement shows that the hot SERS-active sites (enhancement factor $>10^9$) account for only 63 sites over 1 million of the total sites[5]. According to our conservative estimation, the density of the "hot spots" (enhancement factor $>10^9$) in the wrinkled film is thus more than 2 orders of magnitudes higher than that of colloidal particles. Regarding the chemical stability, detectable degradation in the SERS enhancement has not been seen after keeping the wrinkled nanoporous $Au_{79}Ag_{21}$ substrate in ambient environment for more than one month.

In conclusion, we developed a novel nanoporous $Au_{79}Ag_{21}$ substrate with quasi-periodic wrinkles. We observe super enhanced SM-SERS signals from the substrate whatever the probed molecules are resonant or nonresonant with the excitation laser. The enhancement factor for most of the "hot spots" typically reaches up to 10^9, and can be as high as 10^{10}–10^{11} for ~10% of them. The excellent SERS performance of the wrinkled nanoporous $Au_{79}Ag_{21}$ film comes from its heterogeneous nanostructures containing nano-pores, nano-tips, nanogaps and even superlenses, which give the substrate a broad-spectrum of plasmon frequencies for a wide range of molecule detection. The large-scale gold-based SM-SERS substrate with superior

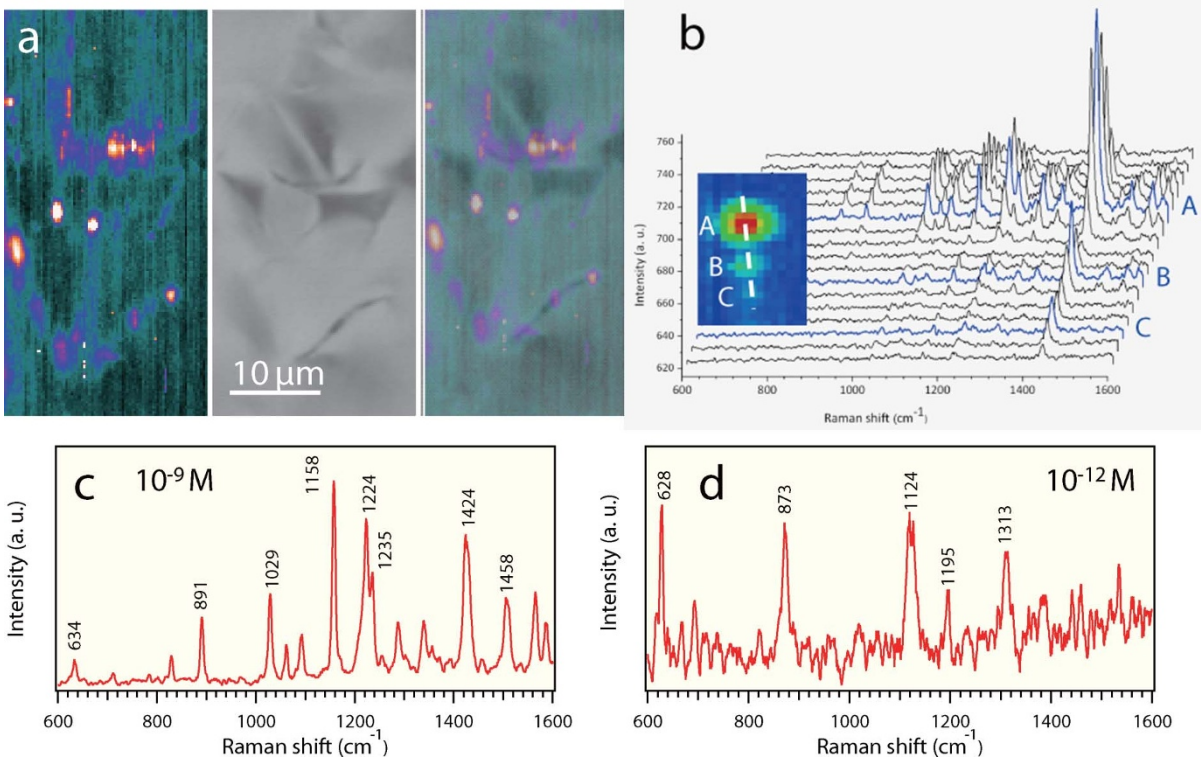

Figure 4 | Single molecule detection of DNA adenine molecules. (a) Typical Raman map of adenine (10^{-9} M) (left), corresponding optical microscopic image (middle), and their overlay image (right). The hot spots can be directly observed at the narrower gaps of the wrinkled nanoporous film. (b) Fluctuation field intensity with 3 chained hot spots (adenine 10^{-9} M). The configuration is analogous to the "superlenses" with a linear chain of nanocavities suggested by computer simulations[30]. Raman map size: 4.0 × 5.5 μm². The spectral interval is 250 nm. (c) SERS spectrum of 10^{-9} M adenine taken from a hot spot. (d) Single molecule SERS spectrum of 10^{-12} M adenine with selective Raman bands. The laser excitation is 785 nm.

reproducibly, facile synthesis and excellent stability may open new avenues for a wide range of applications in life science and environment protection where single molecule detection and identification are critical. Considering the chemical inertness and biocompatibility of the gold-rich alloy, the single-molecule SERS substrate may allow direct visualization of single biomolecules and their assemblies under native physiological conditions for improving our understanding of the behaviour and interaction of individual biological molecules.

Methods

Nanoporous films were prepared by selective dissolution of silver from 100 nm thick $Au_{25}Ag_{75}$ (at. %) leaves in 69% nitric acid[20]. The chemical composition of the dealloyed films was optimized by controlling etching time[31]. The carefully washed nanoporous films were physically attached on pre-strained amorphous polystyrene sheets (PS) (KSF50-C, Grafix). A nanoporous film veneered PS substrate was first baked at 80 °C and subsequently annealed at 160 °C, [26] leading to more than half volume shrinking of the PS. The wrinkled substrate was put in an aqueous solution of the probed molecules and dried in air. We estimate the average surface density of the probed molecules to be ~0.25 per μm^2 of the geometric area of the surface for 1×10^{-12} M solutions (see the Supplementary Methods for more details). Rhodamine 6G (R6G, Aldrich) in aqueous solution and adenine (A, Aldrich) in 0.1 mM NaCl aqueous solution were used as probed molecules for SERS measurements. The structural features of as-prepared and wrinkled $Au_{79}Ag_{21}$ films were investigated by scanning electron microscope (SEM, JIB-4600F). SERS spectra and images were measured using a Nanophoton laser Raman microscope (RAMAN-11) (100×, NA = 0.9). The laser power was set at as low as ~0.1 mW to avoid possible damage from laser irritation.

1. Nie, S. & Emory, S. R. Probing single molecules and single nanoparticles by surface-enhanced Raman scattering. *Science* **275**, 1102–1106 (1997).
2. Kinkhabwala, A. *et al.* Large single-molecule fluorescence enhancements produced by a bowtie nanoantenna. *Nature Photonics* **3**, 654–657 (2009).
3. Celebrano, M., Kukura, P., Renn, A. & Sandoghdar, V. Single-molecule imaging by optical absorption. *Nat. Photon.* **5**, 95–98 (2011).
4. Domke, K. F., Zhang, D & Pettinger, B. Toward Raman fingerprints of single dye molecules at atomically smooth Au(111). *J. Am. Chem. Soc.* **128**, 14721–14727 (2006).
5. Fang, Y., Seong, N.-H. & Dlott, D. D. Measurement of the distribution of site enhancements in surface-enhanced Raman scattering. *Science* **321**, 388–392 (2008).
6. Kneipp, K. *et al.* Single molecule detection using surface-enhanced Raman scattering (SERS). *Phys. Rev. Lett.* **78**, 1667–1669 (1997).
7. Kim, D.-K. *et al.* Nanogap-engineerable Raman-active nanodumbbells for single-molecule detection. *Nat. Mater.* **9**, 60–67 (2010).
8. Kleinman, S. L. *et al.* Single-molecule surface-enhanced Raman spectroscopy of crystal violet isotopologues: theory and experiment. *J. Am. Chem. Soc.* **133**, 4115–4122 (2011).
9. Rodríguez-Lorenzo, L. *et al.* Zeptomol detection through controlled ultrasensitive surface-enhanced Raman scattering. *J. Am. Chem. Soc.* **131**, 4616–4618 (2009).
10. Michaels, A. M., Nirmal, M. & Brus, L. E. Surface enhanced Raman spectroscopy of individual Rhodamine 6G molecules on large Ag nanocrystals. *J. Am. Chem. Soc.* **121**, 9932–9939 (1999).
11. Le Ru, E. C., Meyer, M. & Etchegoin, P. G. Proof of single-molecule sensitivity in surface enhanced Raman scattering (SERS) by means of a two-analyte technique. *J. Phys. Chem. B* **110**, 1944–1948 (2006).
12. Xu, H.-X., Bjerneld, E. J., Käll, M. & Börjesson, L. Spectroscopy of single hemoglobin molecules by surface enhanced Raman scattering. *Phys. Rev. Lett.* **83**, 4357–4360 (1999).
13. Lim, D.-K. *et al.* Highly uniform and reproducible surface-enhanced Raman scattering from DNA-tailorable nanoparticles with 1-nm interior gap. *Nat. Nanotech.* **6**, 452–460 (2011).
14. Li, J. F. *et al.* Shell-isolated nanoparticle-enhanced Raman spectroscopy. *Nature* **464**, 392–395 (2010).
15. Sawai, Y., Takimoto, B., Nabika, H. & Murakoshi, K. Observation of a small number of molecules at a metal nanogap arrayed on a solid surface using surface-enhanced Raman scattering. *J. Am. Chem. Soc.* **129**, 1658–1662 (2007).
16. Hatab, N. A. *et al.* Free-standing optical gold bowtie nanoantenna with variable gap size for enhanced Raman spectroscopy. *Nano Lett.* **10**, 4952–4955 (2010).
17. He, D. *et al.* Large-scale synthesis of flexible free-standing SERS substrates with high sensitivity: Electrospun PVA nanofibers embedded with controlled alignment of silver nanoparticles. *ACS Nano* **3**, 3393–4002 (2009).
18. Ko, H., Chang, S. & Tsukruk, V. V. Porous substrates for lable-free molecular level detection of nonresonant organic molecules. *ACS Nano* **3**, 181–188 (2009).
19. Forty, A. J. Corrosion micromorphology of noble metal alloys and depletion gilding. *Nature* **282**, 597–598 (1979).
20. Erlebacher, J. *et al.* Evolution of nanoporosity in dealloying. *Nature* **410**, 450–453 (2001).
21. Qian, L. H. *et al.* Surface enhanced Raman scattering of nanoporous gold: smaller pore sizes stronger enhancements. *Appl. Phys. Lett.* **90**, 153120 (2007).
22. Kucheyev, S. O. *et al.* Surface-enhanced Raman scattering on nanoporous Au. *Appl. Phys. Lett.* **89**, 053102 (2006).
23. Lang, X. Y. *et al.* Characteristic Length and Temperature Dependence of Surface Enhanced Raman Scattering of Nanoporous Gold. *J. Phys. Chem. C* **113**, 10956–10961 (2009).
24. Bowden, N. *et al.* Spontaneous formation of ordered structures in thin films of metals supported on an elastomeric polymer. *Nature* **393**, 146–149 (1998).
25. Fu, C.-C. *et al.* Tunable nanowrinkles on shape memory polymer sheets. *Adv. Mater.* **21**, 4472–4476 (2009).
26. Zhang, L., Lang, X. Y., Hirata, A. & Chen, M. W. Wrinkled nanoporous gold films with ultrahigh surface-enhanced Raman scattering enhancement. *ACS Nano* **5**, 4407–4413 (2011).
27. Pieczonka, N. P. W. & Aroca, R. F. Single molecule analysis by surfaced-enhanced Raman scattering. *Chem. Soc. Rev.* **37**, 946–954 (2008).
28. Creighton, J. A. Surface Raman electromagnetic enhancement factors for molecules at the surface of small isolated metal spheres: The determination of adsorbate orientation from SERS relative intensities. *Surf. Sci.* **124**, 209–219 (1983).
29. Schuck, P. J. *et al.* Improving the mismatch between light and nanoscale objects with gold bowtie nanoantennas. *Phys. Rev. Lett.* **94**, 017402 (2005).
30. Boriskina, S. V. & Reinhard, B. M. Spectrally and spatially configurable superlenses for optoplasmonic nanocircuits. *Proc. Natl. Acad. Sci.* **108**, 3147–3151 (2011).
31. Zhang, L. *et al.* Effect of residual silver on surface enhanced Raman scattering of dealloyed nanoporous gold. *J. Phys. Chem. C* in press (DOI: 10.1021/jp205892n).

Acknowledgments

This work was sponsored by Grand-in-Aid for Scientific Research (B) (No.21760022), JSPS, fusion research program in WPI-AIMR, and the Global COE for Materials, Research, and Education of the Ministry of Education, Culture, Sports, Science and Technology (MEXT), Japan.

Author contributions

H.W.L., L.Z., Q.K.X. and M.W.C. designed the experiments. H.W.L. and L.Z. performed the experiments and analyzed the data. X.Y.L. contributed in the development of nanoporous metals. Y.Y., H.I. and Y.I. assisted in Raman experiments. H.W.L., Q.K.X. and M.W.C. co-wrote the paper. All authors discussed the results and commented on the manuscript.

Additional information

Supplementary information accompanies this paper at http://www.nature.com/scientificreports

Competing financial interests: The authors declare no competing financial interests.

How to cite this article: Liu, H. *et al.* Single molecule detection from a large-scale SERS-active $Au_{79}Ag_{21}$ substrate. *Sci. Rep.* **1**, 112; DOI:10.1038/srep00112 (2011).